

4. Phases 1 and 2: 85/85 and Thermal Shock

Phase 1 Phase 2

4.1 Introduction. The test matrix in Figure 1.2 shows 160 LRSTF PWAs scheduled for a test sequence consisting of three weeks exposure in an environmental chamber with the temperature and relative humidity set to 85°C at 85%, respectively. This test is followed by a thermal shock (TS) test where all PWAs are rotated between chambers set at $-50^{\circ}\text{C} \pm 5^{\circ}\text{C}$ and $125^{\circ}\text{C} \pm 5^{\circ}\text{C}$. During a single cycle, the PWAs were in one chamber for 30 *min* and were then mechanically rotated into the second chamber for 30 *min*. The test lasted for 200 cycles. Randomization procedures were followed during testing to control extraneous sources of variation—PWAs were placed randomly in the test chamber rack and were tested in a random order to eliminate the effect of possible biases. All electrical testing was performed at the RSC facility in McKinney, TX.

As was true of the previous environmental tests, the 40 urethane PWAs were added to the test matrix after the environmental tests were completed for uncoated, parylene, and silicone coated PWAs. In addition to be tested several months after the other PWAs, the urethane PWAs came from a second build of LRSTF PWAs. The use of a second build introduces an element of uncertainty into the analysis that cannot be resolved with certitude. These facts should be kept in mind when interpreting the urethane results as effects apparently due to urethane, could be reflecting different test times or differences in builds or batches of components. There is no way to know for sure. (See the extended discussion in Section 2.1.)

4.2 Overview of Test Results. The 160 PWAs in the 85/85-TS test sequence were tested at the following times:

- Pre-test
- After week 1 of 85/85
- After week 2 of 85/85
- After week 3 of 85/85 (Post-test)
- After 100 cycles of TS
- After 200 cycles of TS

At each of these test times, $160 \times 23 = 3680$ electrical test measurements were recorded. An overview of the test results at each test time is now given. Detailed results of the electrical performance for each of the 23 circuits listed in Table 1.1 appear in Sections 4.3 to 4.9. Summary and conclusions appear in Section 4.10.

Pre-test. Electrical measurements are compared to the JTP acceptance criteria given in Table 1.1 at each test time. These acceptance criteria require a comparison to Pre-test for 11 of the 23 electrical circuits (#'s 1, 2, 5, 6, 13-17, 22, and 23). This group of 11 circuits was compared with historical performance data while the remaining $23 - 11 = 12$ circuits were compared directly to the JTP acceptance criterion.

The 12 electrical circuits that were compared to the JTP acceptance criteria produced $12 \times 160 = 1920$ Pre-test measurements. Eleven anomalies in these measurements did not meet their respective JTP acceptance criterion. Of these 11, three gave normal responses at all subsequent test times, so their Pre-test measurements were most likely erroneous. Two of the remaining anomalies occurred on a single PWA for HSD PTH and HSD SMT (circuits 5 and 6 in Table 1.1), which were most likely due to component damage or trace damage that plague the HSD circuits with regularity. The remaining six anomalies occurred for HF LPF circuits on three PWAs (circuits 8, 9, 11, and 12 in Table 1.1). These circuits remained just above the upper acceptance limit throughout subsequent test times. Without the three suspect measurements, the percentage of PWAs meeting the JTP acceptance criteria at Pre-test was $1912/1920 = 99.6\%$.

Week 1 of 85/85. There were 33 measurements on 19 PWAs that did not meet the JTP acceptance criteria at Week 1. Eight of these anomalies were on a single PWA. These eight circuits did not have any anomalous measurements at subsequent test times, which casts doubt on the validity of these measurements at Week 1. Without these eight suspect measurements, the percentage of measurements meeting the JTP acceptance criteria at Week 1 was $3655/3680 = 99.3\%$. All 33 anomalies for Week 1 are categorized in Table 4.1 by surface finish, coating status, and flux type (suspect measurements appear in parentheses). The following summary of the 19 PWAs that had anomalies does not indicate any association between the number of anomalies and the experimental parameters: surface finish (HASL, benzimidazole, immersion Ag, or immersion Au/Pd), coating status (no coating, parylene, silicone, or urethane), or flux type (LR or WS).

Surface Finish		Coating Status		Flux Type	
HASL	4	None	5	Low-residue	10
Benzimidazole	4	Parylene	5	Water soluble	9
Immersion Ag	8	Silicone	3		
Immersion Au/Pd	3	Urethane	6		

Week 2 of 85/85. There were only 13 measurements on nine PWAs that did not meet the JTP acceptance criteria at Week 2. The percentage of measurements meeting the JTP acceptance criteria at Week 2 was 3667/3680 = 99.6%. All 13 anomalies for Week 2 are categorized in Table 4.2 by surface finish, coating status, and flux type. The nine PWAs having anomalies are summarized as follows.

Surface Finish		Coating Status		Flux Type	
HASL	1	None	4	Low-residue	7
Benzimidazole	1	Parylene	1	Water soluble	2
Immersion Ag	6	Silicone	2		
Immersion Au/Pd	1	Urethane	2		

A chi-square test of independence (see Iman, 1994) shows that immersion Ag has significantly more anomalies than the other surface finishes (p -value = 0.032) after Week 2. This same test does not indicate any significant differences for coating status or flux type. The p -value is a measure of statistical significance and should be < 0.05 to declare a statistical difference.

Week 3 or 85/85 (Post-test). At the conclusion of the 85/85 test there were 33 anomalies on 26 PWAs that did not meet the JTP acceptance criteria, which gave a yield of 3647/3680 = 99.1%. The number of anomalies at Post-test increased by 20 over Week 2 of the 85/85 test. Two circuit groups were primarily responsible for this increase. HVLC had eight more anomalies and leakage had 10 more. In addition, the number of HSD circuits not giving a response increased from eight to 22. Failure analyses have previously shown that HSD anomalies on the LRSTF PWA are caused by either component damage or trace damage due to electrical overstress. Two of the HVLC anomalies could not be duplicated during failure analysis following the conclusion of the 85/85 test and the rest were due to either open resistors or an open circuit trace. These anomalies occurred for all surface finishes, coating conditions, and flux types. Detailed results for these four circuits are given in Sections 4.5 to 4.8. Table 4.3 tabulates all 33 anomalies by surface finish, coating status, and flux type. The 26 PWAs having anomalies are summarized as follows.

Surface Finish		Coating Status		Flux Type	
HASL	8	None	14	Low-residue	15
Benzimidazole	4	Parylene	3	Water soluble	11
Immersion Ag	10	Silicone	4		
Immersion Au/Pd	4	Urethane	5		

A chi-square test of independence shows there are significantly more anomalies for uncoated PWAs than for the coated PWAs. This same test does not indicate any significant differences for surface finishes (as was true after Week 2) or flux type.

Of the 33 anomalous measurements, 16 were severe enough to be candidates for further investigation with failure analysis to determine the cause of the anomaly. These 16 candidates were distributed by circuit type as follows: HVLC PTH (4), HVLC SMT (4), leakage (2), HF LPF (4), and HF TLC (2).

100 Cycles of Thermal Shock. There were 46 anomalies that did not meet the JTP acceptance criteria after 100 cycles of TS, which is an increase of 13 from the number observed at the conclusion of the 85/85 test. Table 4.4 tabulates all 46 anomalies by surface finish, coating status, and flux type. These 46 anomalous measurements occurred on 28 PWAs. The surface finishes, coating conditions, and flux types for these 28 PWAs are summarized as follows:

Surface Finish		Coating Status		Flux Type	
HASL	7	None	11	Low-residue	15
Benzimidazole	4	Parylene	4	Water soluble	13
Immersion Ag	9	Silicone	6		
Immersion Au/Pd	8	Urethane	7		

Table 4.1 Tabulation of the 25 (33) Test Measurements Over All 23 Electrical Circuits that did not Meet the JTP Acceptance Criteria at Week 1 of the 85/85 test (numbers in parentheses represent questionable measurements on a single PWA)

		No Coating	Parylene	Silicone	Urethane	Totals
HASL (4)	LR	1				1
	WS				3	3
Benzimidazole (6)	LR		1(8)		4	5(8)
	WS		1			1
Immersion Ag (10)	LR		2	3	1	6
	WS	2	1	1		4
Imm. Au/Pd (5)	LR	2				2
	WS				3	3
LR= 14, WS=11	Totals	5	5(8)	4	11	25(8)

Table 4.2 Tabulation of the 13 Test Measurements Over All 23 Electrical Circuits that did not Meet the JTP Acceptance Criteria at Week 2 of the 85/85 test

		No Coating	Parylene	Silicone	Urethane	Totals
HASL (1)	LR				1	1
	WS					
Benzimidazole (1)	LR					
	WS	1				1
Immersion Ag (8)	LR	1	2	3	1	7
	WS	1				1
Imm. Au/Pd (3)	LR	3				3
	WS					
LR= 11, WS=2	Totals	6	2	3	2	13

Table 4.3 Tabulation of the 33 Test Measurements Over All 23 Electrical Circuits that did not Meet the JTP Acceptance Criteria at Week 3 (Post-test) of the 85/85 Test

		No Coating	Parylene	Silicone	Urethane	Totals
HASL (10)	LR	1		2	0	3
	WS	4	1	1	1	7
Benzimidazole (4)	LR	1		1		2
	WS	2				2
Immersion Ag (13)	LR	2	2	2	3	9
	WS	2	2			4
Imm. Au/Pd (6)	LR	5			1	6
	WS					
LR= 20, WS=13	Totals	17	5	6	5	33

Table 4.4 Tabulation of the 46 Test Measurements Over All 23 Electrical Circuits that did not Meet the JTP Acceptance Criteria after 100 Cycles of Thermal Shock

		No Coating	Parylene	Silicone	Urethane	Totals
HASL (14)	LR	1			3	4
	WS	3	1	1	5	10
Benzimidazole (9)	LR				3	3
	WS	6				6
Immersion Ag (12)	LR	1	2	3	1	7
	WS	2	2	1		5
Imm. Au/Pd (11)	LR	4	1	1	2	8
	WS			3		3
LR= 22, WS=24	Totals	17	6	9	14	46

Table 4.5 Tabulation of the 42 Test Measurements Over All 23 Electrical Circuits that did not Meet the JTP Acceptance Criteria after 200 Cycles of Thermal Shock

		No Coating	Parylene	Silicone	Urethane	Totals
HASL (6)	LR	1				1
	WS	2	1	1	1	5
Benzimidazole (3)	LR					
	WS	2			1	3
Immersion Ag (14)	LR	1	2	2	3	8
	WS	2	2		2	6
Imm. Au/Pd (11)	LR	4	3			7
	WS			3	1	4
LR= 16, WS=19	Totals	12	8	6	8	34

A chi-square test of independence does not indicate any significant differences for surface finishes, coating status, or flux type after 100TS.

200 Cycles of Thermal Shock. At the end of 200 cycles of thermal shock, the number of electrical measurements not meeting the JTP acceptance decreased to 34 from TS100. Thus, $3646/3680 = 99.1\%$ of the circuits tested survived the 85/85—thermal shock sequence. The 34 anomalies occurred on 25 of the 160 PWAs. Table 4.5 gives a tabulation of all 34 anomalies by surface finish, coating status, and flux type. This tabulation shows that immersion Ag had the most anomalies with 14. Eight of the immersion Au/Pd anomalies were attributable to multiple HF problems on just three PWAs. The 25 PWAs having anomalies are summarized as follows.

Surface Finish	Coating Status	Flux Type
HASL	6 None	11 Low-residue
Benzimidazole	3 Parylene	4 Water soluble
Immersion Ag	10 Silicone	3
Immersion Au/Pd	6 Urethane	7

A chi-square test of independence does not indicate any significant differences for surface finishes, coating status, or flux type after 200TS.

Table 4.6 summarizes all anomalies that did not meet the JTP acceptance criteria for each circuit at each test time. This table is helpful in tracking the changes in circuit behavior over time.

Table 4.6 Anomalies That Did Not Meet JTP Acceptance Criteria at Weeks 1, 2, and 3 (Post-Test) of the 85/85 Test Environment and after 100 and 200 Cycles of Thermal Shock (tabulated by electrical circuit)

Electrical Response:	HCLV	HVLC	HSD	HF LPF					HF TLC				Leakage			SW				
Test Time	HCLV PTH HCLV SMT	HVLC PTH HVLC SMT	HSD PTH HSD SMT	HF PTH 50 Mhz	HF PTH f(-3dB)	HF PTH f(-40 dB)	HF SMT 50 Mhz	HF SMT f(-3dB)	HF SMT f(-40 dB)	HF TLC 50 MHz	HF TLC 500 MHz	HF TLC 1GHz	HF TLC Rev Null Freq	HF TLC Rev Null Resp	10-Mil Pads	PGA-A	PGA-B	Gull Wing	Stranded Wire 1	Stranded Wire 2
Week 1	4	3	1	3	3	1	2	3	4	2	1	1	4					1		
Week 2		1	1		2	2	1	1	1				2					2		
Post-Test	1	5	5		2	2	1	1	3				1	1	1	4	6			
100 Cycles	4	5	5	2	1				4	2	1	2	2	3	3	2	2	3	1	4
200 Cycles	1	5	5		1	3	3	1	2	2	3		4	1			3			

4.3 HCLV Circuitry. Table 4.7 (also presented as Table E.1 in Appendix E) shows the statistically significant coefficients in the GLM in Equation 1.1 (see Section 1.8) for the voltage measurements on the HCLV PTH circuitry at Pre-test and for the following differences between successive test times:

- Delta 1 = Week 1 - Pre-test
- Delta 2 = Week 2 - Pre-test
- Delta 3 (Post-Delta) = Post-test - Pre-test
- Delta 4 = 100TS - Pre-test
- Delta 5 = 200TS - Pre-test

Appendix E contains the GLM results for each of the 23 electrical responses measured on the LRSTF PWA. Since each summary table fills one page, these tables have been placed in Appendix E for ease of reference and to improve the readability of this section. Subsequent discussions of the GLM results for the remaining circuitry make reference to Tables E.1 to E.23. Pre-test measurements for the HCLV circuits were subjected to GLM analyses, as were the deviations Delta 1 to Delta 5. The results of the GLM analyses for HCLV are given in Tables E.1 and E.2. The model R²s from those tables are summarized as follows.

HF LPF Circuit	Pre-test	Week 1	Week 2	Post	100TS	200TS
HCLV PTH	15.1%	3.2%	7.9%	5.0%	2.9%	2.5%
HCLV SMT	25.9%	7.5%	0.6%	27.3%	13.1%	10/7%

These low R² values imply that the experimental parameters do not differ significantly from the base case in terms of their impact on the HCLV circuitry. That is, there is no difference from the base case voltage measurements due to surface finishes, coating status (i.e., no coating, parylene, or silicone), or flux type.

Displays. Appendix F presents boxplots (see Section 1.9) for each of the 23 electrical responses measured on the LRSTF PWA. Since each set of graphs for a given response requires two pages (46 pages in all), these graphs have been placed in Appendix F for ease of reference and to improve the readability of this section. Subsequent discussions of graphical displays for the remaining circuitry make reference to Figures F.1 to F.92.

Figure F.1 presents boxplots for the HCLV PTH voltage measurements for the HASL surface finish. These measurements are plotted versus test time with LR flux results on the left and WS results on the right. Four overlapping boxplots are used at each test time to show the effect of coating status. Note that the measurements exhibit approximately the same amount of variability throughout and that the voltages in these figures vary over a reasonably small range of 6.7V to 7.4V. Figures F.2, F.3, and F.4 give similar results for benzimidazole,

Table 4.7 Significant Coefficients for the GLM Analyses by Test Time for HCLV PTH

Electrical Response: HCLV PTH	85/85				Thermal Shock	
	Pre-Test	Delta 1	Delta 2	Post-Delta	100 Cycles	200 Cycles
Constant	6.963	0.026	-0.019	0.010	-0.003	0.009
Benzimidazole Immersion Ag Immersion Au/Pd						
Parylene Silicone Urethane	0.160					
Flux		-0.086				
Benzi*Parylene Imm Ag*Parylene Imm Au/Pd*Parylene				0.278		
Benzi*Silicone Imm Ag*Silicone Imm Au/Pd*Silicone			-0.205			-0.137
Benzi*Urethane Imm Ag* Urethane Imm Au/Pd* Urethane						
Benzi*Flux Imm Ag*Flux Imm Au/Pd*Flux						
Parylene*Flux Silicone*Flux Urethane*Flux						
Benzi*Parylene*Flux Imm Ag*Parylene*Flux Imm Au/Pd*Parylene*Flux				-0.320		
Benzi*Silicone*Flux Imm Ag*Silicone*Flux Imm Au/Pd*Silicone*Flux						
Benzi*Urethane*Flux Imm Ag*Urethane*Flux Imm Au/Pd*Urethane*Flux			-0.237		-0.213	
Model R ²	15.1%	3.2%	7.9%	5.0%	2.9%	2.5%
Standard Deviation	0.165	0.240	0.217	0.217	0.218	0.210

immersion Ag, and immersion Au/Pd, respectively. Figures F.5 to F.8 present boxplots for the HCLV SMT voltage measurements versus test time for HASL, benzimidazole, immersion Ag, and immersion Au/Pd, respectively. Note that the voltages in these figures vary over a reasonably small range of 7.00V to 7.35V.

Comparison to JTP Acceptance Criterion. All HCLV PTH and HCLV SMT measurements were well below the JTP acceptance criterion of $\Delta V < 0.50V$ after three weeks of 85/85 exposure. There was only one slight anomaly after 200TS ($\Delta V = 0.56V$), which did not require failure analysis.

4.4 HVLC Circuitry. Tables E.3 and E.4 show the statistically significant coefficients in the GLM in Equation 1.1 for the current (μA) measurements on the HVLC PTH and HVLC SMT circuits at Pre-test, Week 1, Week 2, Post-test, 100TS and 200TS. Note that no deltas calculated for these measurements. The GLMs for Post-test, 100TS and 200TS did not use data for the anomalies listed in Table 4.8. The model R^2 's given in Tables E.3 and E.4 are summarized as follows.

HF LPF Circuit	Pre-test	Week 1	Week 2	Post	100TS	200TS
HVLC PTH	20.1%	52.0%	31.0%	26.6%	0.6%	0.5%
HVLC SMT	61.9%	21.1%	58.7%	40.8%	58.7%	58.5%

Even though some of the HVLC model R^2 's were of moderate size, the magnitude of the coefficients in each of these models was too small to be of practical concern relative to the JTP acceptance criterion. Thus, none of the experimental parameters have any practical effect on the performance of the HVLC PTH circuit relative to the JTP acceptance criterion.

Displays. Figures F.9 to F.12 present boxplots for the HVLC PTH current measurements versus test time for HASL, benzimidazole, immersion Ag, and immersion Au/Pd, respectively. The boxplots have approximately the same degree of variability throughout with a few exceptions mostly associated with parylene. However, even the most extreme variation for parylene has a range of less than $0.2\mu\text{A}$. At the conclusion of the TS test all results are similar (their combined range is only from $4.92\mu\text{A}$ to $5.25\mu\text{A}$). The corresponding boxplots for HVLC SMT appear in Figures F.13 to F.16. These boxplots show that urethane coated PWAs have the greatest variability throughout, however, even the most extreme variation for urethane has a range of less than $0.15\mu\text{A}$. At the conclusion of the TS test all results are similar (their combined range is only from $4.92\mu\text{A}$ to $5.13\mu\text{A}$). The reader should keep in mind that the JTP acceptance criterion specifies an acceptable range from $4\mu\text{A}$ to $6\mu\text{A}$. The graphs in Figures F.9 to F.16 have been enlarged and show only a small portion of that acceptable range where the actual current measurements occurred.

Comparison to JTP Acceptance Criterion. There were six anomalous HVLC PTH measurements that did not meet the JTP acceptance criterion after 200TS. Four of these six circuits previously gave anomalous readings at Post-test and failure analysis was performed at that time. These failure analysis results are summarized by surface finish, coating status, and flux type in Table 4.8. One of these six anomalies was just above the upper acceptance limit at $6.20\mu\text{A}$ and was not of concern with respect to failure analysis. The remaining anomaly was attributable to a broken P1 connector at TS200 that did not allow measurements to be recorded for the HVLC and leakage circuits. Since these circuits were normal at TS100, it was assumed that they still functioned properly at TS200. The range of 153 of the remaining 154 HVLC PTH measurements was $4.86\mu\text{A}$ to $5.05\mu\text{A}$ with one additional value at $5.49\mu\text{A}$. All of these 154 measurements were well within the JTP acceptance criterion. Based on failure analysis results in Table 4.8, it is unlikely that there is any relationship between these failures and board processes (surface finish, coating status, or flux type).

There were also six anomalous HVLC SMT measurements that did not meet the JTP acceptance criterion after 200TS. Five of these six circuits previously gave anomalous readings at Post-test and failure analysis was performed at that time. Those failure analysis results are summarized by surface finish, coating status, and flux type in Table 4.8. Note that the PWAs with HVLC SMT anomalies are different from those involved in the failure analysis for HCLV PTH. As with HVLC PTH, there was one additional anomaly that was attributable to a broken P1 connector at TS200 that did not allow measurements to be recorded for the HVLC SMT circuit. Since this circuit was normal at TS100, it was assumed that it still functioned properly at TS200. The range of 152 of the remaining 154 measurements was only $4.93\mu\text{A}$ to $5.12\mu\text{A}$ with two additional values at $5.40\mu\text{A}$ and $5.67\mu\text{A}$, all of which are well within the JTP acceptance criterion.

As shown in Table 4.8, four HVLC SMT anomalies were due to open circuit traces, which were caused by a bleed-over of the 250V to an adjacent conductor (e.g., V_{cc} or ground). This bleed-over eventually caused current high enough to fuse open the metal traces. The anomaly on the fifth PWA could not be duplicated, although there is evidence of arcing on it as well. The SMT portion of the HVLC circuitry is more susceptible to arcing than the PTH portion since there are more adjacent low potential traces next to the 250V SMT line than for the 250V PTH line. Based on failure analysis results, it is unlikely there is any relationship between these failures and board processes (surface finish, coating status, or flux type).

4.5 HSD Circuitry. Tables E.5 and E.6 show the statistically significant coefficients in the GLM in Equation 1.1 for total propagation delay (*nanoseconds*) measurements on the HSD PTH circuitry at Pre-test and for Deltas 1 to 5.

Table 4.8 Failure Analysis Results for HVLC Circuits after 200 Cycles of Thermal Shock

MSN	Surface Finish	Coating	Flux	Current	Failure Analysis Results
HVLC PTH					
16	HASL	None	LR	0.20 μ A	Open resistor
324	HASL	None	WS	0.56 μ A	Open resistor
354	HASL	Silicone	WS	6.20 μ A	FA not required
379	Benzimidazole	None	WS	0.23 μ A	Open resistor
490	Immersion Ag	Parylene	WS	0 μ A	Could not duplicate; evidence of arcing at 250V line on input connector
HVLC SMT					
343	HASL	Parylene	WS	1.18 μ A	Could not duplicate
161	Immersion Ag	None	LR	8.30 μ A	Open circuit trace
474	Immersion Ag	None	WS	0 μ A	Open circuit trace
247	Imm. Au/Pd	None	LR	0 μ A	Open circuit trace
229	Imm. Au/Pd	None	LR	0 μ A	Open circuit trace

The deltas are defined as the percentage change from the Pre-test measurements. As was explained in Section 2.5, Pre-test measurements for the urethane PWAs showed that TPD was approximately 4ns longer for these PWAs than for the non-urethane PWAs. Though the TPD is longer, the same JTP acceptance criterion (increase in TPD < 20%) was applied to both groups of PWAs.

The GLMs for Post-test, 100TS, and 200TS did not use data for the anomalies listed in Table 4.9. The model R^2 's from the GLM analyses in Tables E.5 and E.6 are summarized as follows.

HF LPF Circuit	Pre-test	Week 1	Week 2	Post	100TS	200TS
HSD PTH	99.1%	13.6%	1.1%	14.5%	10.9%	11.2%
HSD SMT	99.4%	5.1%	9.3%	0.8%	12.6%	3.4%

Since the GLM analyses at Pre-test were based on the actual TPDs, the high R^2 values at Pre-test simply reflect the differences in the TPD for urethane versus the non-urethane PWAs (see Section 2.5). After Pre-test, the GLM analyses were based on the percentage change in TPD. The model R^2 values are all quite small for the remaining test times, which implies that the experimental parameters did not differ significantly from the base case in terms of their impact on the HSD circuits. That is, there is no practical difference from the base case TPD measurements due to surface finishes, coating status, or flux type. The coefficients in Tables E.5 and E.6 were too small to be of concern relative to the JTP acceptance criterion.

Displays. Figures F.17 to F.20 present boxplots for the HSD PTH propagation delay measurements (without the anomalies listed in Table 4.9) versus test time for HASL, benzimidazole, immersion Ag, and immersion Au/Pd, respectively. These boxplots reflect the difference in TPD due to the use of different HSD components on the urethane PWAs. Note that the range of TPD reflected in the individual boxplots in these figures is generally less than 1 nsec. The boxplots show similar behavior throughout, except for two or three cases having a couple of outlying observations.

Figures F.21 to F.24 present boxplots for the HSD SMT propagation delay measurements (without the anomalies listed in Table 4.9) versus test time for HASL, benzimidazole, immersion Ag, and immersion Au/Pd, respectively. These boxplots reflect the difference in TPD due to the use of different HSD components on the urethane PWAs. Note that the range of TPD reflected in the individual boxplots in these figures is generally less than 1 nsec. The boxplots show similar behavior throughout.

Comparison to JTP Acceptance Criterion. There were no anomalous HSD PTH measurements that exceeded the JTP acceptance criterion after 200TS, but there were 10 circuits for which no meaningful measurements were recorded. Nine of these 10 additional circuits did not have responses for HSD SMT, which implies the HSD PTH and SMT anomalies are not independent of one another. That is, if the HSD PTH component fails, the HSD SMT component also fails. These PWAs were all subjected to failure analysis. Failure analysis results are summarized by surface finish, coating status, and flux type in Table 4.9. Eight of the 10 HSD PTH anomalies first

Table 4.9 Failure Analysis Results for HSD Circuits after 200 Cycles of Thermal Shock

MSN	Surface Finish	Coating	Flux	Failure Analysis Results
HSD PTH				
366	HASL	Silicone	WS	Component damage
604	HASL	Urethane	LR	
673	HASL	Urethane	WS	
137	Benzimidazole	Silicone	LR	
445	Benzimidazole	Silicone	WS	Component damage
760	Benzimidazole	Urethane	WS	
491	Immersion Ag	Parylene	WS	Component damage
217	Immersion Ag	Silicone	LR	Component damage
263	Immersion Au/Pd	Parylene	LR	Component damage
863	Immersion Au/Pd	Urethane	LR	
HSD SMT				
321	HASL	None	WS	Component damaged
324	HASL	None	WS	Trace damaged
362	HASL	Parylene	WS	Trace damaged
366	HASL	Silicone	WS	Component damaged
604	HASL	Urethane	LR	
380	Benzimidazole	None	WS	Trace damaged
137	Benzimidazole	Silicone	LR	Component damaged
445	Benzimidazole	Silicone	WS	Trace damaged
760	Benzimidazole	Urethane	WS	
469	Immersion Ag	None	WS	Trace damaged
491	Immersion Ag	Parylene	WS	Trace damaged
217	Immersion Ag	Silicone	LR	Trace damaged
247	Immersion Au/Pd	None	LR	Trace damaged
229	Immersion Au/Pd	None	LR	Trace damaged
548	Immersion Au/Pd	None	WS	Trace damaged
263	Immersion Au/Pd	Parylene	LR	Component damaged
863	Immersion Au/Pd	Urethane	LR	

occurred at Post-test of 85/85. These 10 failures included all four surface finishes and were evenly split between LR and WS flux. All 10 anomalies were conformally coated: parylene (2), silicone (4), and urethane (4). Failure analysis revealed that all the damage sustained in the HSD PTH section was due to electrical overstress (EOS), which damaged either the active components or the circuit traces. The source of the EOS was likely from the adjacent Other Networks (leakage current) section of the PWA, which was biased with 100V.

Table 4.9 also lists 17 anomalous HSD SMT circuits for which no meaningful measurements were recorded after 200TS (12 of these circuits gave no meaningful measurements following Post-test of the 85/85 test). Failure analysis results are summarized by surface finish, coating status, and flux type in Table 4.9. Nine of these 17 PWAs were also subjected to failure analysis for the HSD PTH circuitry, which implies that the HSD PTH and SMT failures are not independent of one another. These 17 HSD SMT anomalies included all surface finishes: HASL (5), benzimidazole (4), immersion Ag (3), and immersion Au/Pd (5). Seven of the 17 were processed with LR flux and the remaining 10 with WS flux. The anomaly summary by coating status is as follows: none (7), parylene (3), silicone (4), and urethane (3).

As was the case for HSD PTH, failure analysis revealed that all the damage sustained in the HSD section was due to electrical overstress (EOS), which damaged either the active components or the circuit traces. The source of the EOS was likely from the adjacent Other Networks (leakage current) section of the PWA, which was biased with 100V.

The combined 27 HSD PTH and HSD SMT anomalies listed in Table 4.9 occurred on 18 PWAs. These PWAs show no evidence of being associated with any particular experimental conditions (surface finish, coating status, or flux), as they were evenly spread over surface finishes, coating status, and flux type as follows.

Surface Finish		Coating Status		Flux Type	
HASL	6	None	7	Low-residue	7
Benzimidazole	4	Parylene	3	Water soluble	11
Immersion Ag	3	Silicone	4		
Immersion Au/Pd	5	Urethane	4		

4.6 HF LPF Circuitry. The JTP acceptance criteria for HF LPF PTH 50MHz and HF LPF SMT 50MHz (responses 7 and 10 in Table 1.1) are based on deviations from the average response of the five HASL PWAs coated with parylene and processed with LR flux at the current test time. Specifically, these deviations must be within ± 5 dB of this average.

The JTP acceptance criteria for HF LPF PTH f(-3dB), HF LPF PTH f(-40dB), HF LPF SMT f(-3dB), and HF LPF SMT f(-40dB) (responses 8, 9, 11, and 12 in Table 1.1) are also based on deviations from the average response of the five HASL PWAs coated with parylene and processed with LR flux at the current test time. Specifically, these deviations must be within ± 50 MHz of this average.

Pre-test measurements for all six HF LPF circuits were subjected to GLM analyses, as were the deviations Delta 1 to Delta 5. The results of the GLM analyses are given in Tables E.7 to E.12. The model R^2 s in those tables are summarized as follows.

HF LPF Circuit	Pre-test	Week 1	Week 2	Post	100TS	200TS
PTH 50MHz	10.9%	26.3%	27.9%	29.1%	16.7%	32.4%
PTH f(-3dB)	20.8%	15.6%	23.1%	17.0%	27.5%	22.5%
PTH f(-40dB)	23.8%	19.2%	24.0%	29.4%	25.8%	23.4%
SMT 50MHz	5.9%	18.3%	20.3%	10.8%	28.3%	38.0%
SMT f(-3dB)	19.3%	16.5%	25.4%	14.1%	21.5%	21.1%
SMT f(-40dB)	20.1%	32.4%	40.7%	40.0%	18.4%	38.6%

These model R^2 s range from quite small to 40%. However, the estimated coefficients in all models were too small to be of practical significance relative to the JTP acceptance criteria. Hence, surface finish, coating status, and flux type do not have any practical influence on the HF LPF circuitry. The GLM analyses did not include the anomalous measurements listed in Table 4.10.

Displays. Figures F.25 to F.28 present boxplots for the HF LPF PTH 50MHz response function measurements versus test time for HASL, benzimidazole, immersion Ag, and immersion Au/Pd, respectively. These figures show that the responses were essentially the same for all combinations of experimental parameters after 200TS.

Figures F.29 to F.32 present boxplots for the HF LPF PTH f(-3dB) measurements (without the largest anomalies discussed below) versus test time for HASL, benzimidazole, immersion Ag, and immersion Au/Pd, respectively. The boxplots in these figures show different degrees of variability but are generally within a 20MHz range from 240MHz to 260MHz.

Figures F.33 to F.36 present boxplots for the HF LPF PTH f(-40dB) measurements (without the largest anomalies discussed below) versus test time for HASL, benzimidazole, immersion Ag, and immersion Au/Pd, respectively. The boxplots in these figures show different degrees of variability but are generally within a 20MHz range from 425MHz to 450MHz.

Figures F.37 to F.40 present boxplots for the HF LPF SMT 50MHz response function measurements versus test time for HASL, benzimidazole, immersion Ag, and immersion Au/Pd, respectively. These figures show that the responses were essentially the same for all combinations of experimental parameters after 200TS.

Figures F.41 to F.44 present boxplots for the HF LPF SMT f(-3dB) measurements (without the two anomalies listed below) versus test time for HASL, benzimidazole, immersion Ag, and immersion Au/Pd, respectively. The boxplots in these figures have about a 5MHz range for most cases.

Figures F.45 to F.48 present boxplots for the HF LPF SMT f(-40dB) measurements (without the two anomalies discussed below) versus test time for HASL, benzimidazole, immersion Ag, and immersion Au/Pd, respectively. The boxplots in these figures have a range of about 10 to 20MHz for most cases.

Table 4.10 Failure Analysis Results for HF LPF Circuits after 200 Cycles of Thermal Shock

MSN	Surface Finish	Coating	Flux	Deviation	Failure Analysis Results
HF LPF PTH 50MHZ					
251	Immersion Au/Pd	Parylene	LR	-26.8dB	Open via due to over etching of the copper hole
HF LPF PTH f(-3dB)					
251	Immersion Au/Pd	Parylene	LR	-204.6MHz	Open via due to over etching of the copper hole
184	Immersion Ag	Parylene	LR	55.5MHz	Failure analysis not required
217	Immersion Ag	Silicone	LR	53.7MHz	Failure analysis not required
HF LPF PTH f(-40dB)					
184	Immersion Ag	Parylene	LR	68.8MHz	Failure analysis not required
217	Immersion Ag	Silicone	LR	66.4MHz	Failure analysis not required
251	Immersion Au/Pd	Parylene	LR	406.6MHz	Open via due to over etching of the copper hole
HF LPF SMT 50MHz					
596	Immersion Au/Pd	Silicone	WS	-46.1dB	Open via
HF LPF SMT f(-3dB)					
596	Immersion Au/Pd	Silicone	WS	-228.1MHz	Open via
238	Immersion Au/Pd	None	LR	110.3MHz	Open solder joint on a chip capacitor
HF LPF SMT f(-40dB)					
596	Immersion Au/Pd	Silicone	WS	-542.1MHz	Open via
238	Immersion Au/Pd	None	LR	220.9MHz	Open solder joint on a chip capacitor

Comparison to JTP Acceptance Criterion. After 200TS there were 12 anomalies on five PWAs that did not meet the JTP acceptance criteria for HF LPF circuits. Four of these anomalies were just above the upper limit of the acceptance criterion and were not of concern. Failure analyses were conducted on the remaining eight anomalies (three PWAs) at Post-test of the 85/85 test (where they first occurred). These results summarized in Table 4.10 show two anomalies were due to an open solder joint on a chip capacitor and the remainder were due to an open via. Note that all PWAs with severe anomalies had an immersion Au/Pd surface finish.

4.7 HF TLC Circuitry. The JTP acceptance criteria for HF TLC circuitry (responses 13 to 17 in Table 1.1) are all based on changes from their Pre-test measurements. The changes for HF TLC 50MHz, HF TLC 500MHz, and HF TLC 1GHz must be within ± 5 dB of the Pre-test values. The changes for HF TLC Reverse Null Frequency must be within ± 50 MHz. Finally, the changes for HF TLC Reverse Null Response must be less than 5dB if both responses are greater than -50dB, otherwise they must be less than 10dB.

Pre-test measurements for all five HF TLC circuits were subjected to GLM analyses, as were the deviations Delta 1 to Delta 5. The results of the GLM analyses are given in Tables E.13 to E.17. The model R^2 s in those tables are summarized as follows.

HF TLC Circuit	Pre-test	Week 1	Week 2	Post	100TS	200TS
50MHz	76.1%	21.6%	25.6%	36.2%	17.2%	24.5%
500MHz	87.4%	14.3%	15.9%	22.1%	29.7%	20.6%
1GHz	76.1%	7.9%	3.8%	5.5%	3.7%	12.0%
RNF	81.7%	24.9%	52.6%	17.5%	62.6%	40.2%
RNR	17.7%	1.3%	3.1%	1.4%	10.8%	27.5%

The model R^2 s at Pre-test are high for the first four HF TLC circuits. The magnitudes of these R^2 s are attributable to the different electrical properties of conformal coatings as previously discussed in Section 2.7. The model R^2 s for the deltas range from quite small to close to 63%. However, the estimated coefficients in all models were too

small to be of practical significance relative to the JTP acceptance criteria, which indicates the impact of surface finish, coating status, and flux type on HF TLC was not of concern.

Displays. Figures F.49 to F.52 present boxplots for the HF TLC 50MHz measurements versus test time for HASL, benzimidazole, immersion Ag, and immersion Au/Pd, respectively. Since these boxplots utilize the raw test measurements (rather than deltas), they show the distinct effect due to coating that was alluded to in the above discussion. The average HF TLC 50MHz responses by coating status are: none (-37.87dB), parylene (-38.72dB), silicone (-42.98dB), and urethane (-40.11dB).

Figures F.53 to F.56 present boxplots for the HF TLC 500MHz measurements versus test time for HASL, benzimidazole, immersion Ag, and immersion Au/Pd, respectively. Note the change in the vertical scale compared to Figures F.49 to F.52. As was the case at 50MHz, the boxplots in these figures show a distinct effect due to coating status. The average HF TLC 500MHz responses by coating status are: none (-18.97dB), parylene (-19.99dB), silicone (-21.66dB), and urethane (-20.45dB). These means are less than half those observed at the 50MHz point on the high frequency forward response function. There are two reasons for these smaller differences. First, the forward response function is flatter at 500MHz than at 50MHz, which means there is less variability in the vertical direction for these measurements. The second factor is that the test equipment has better resolution at 500MHz (range of response: -22dB to -17dB) than at 50MHz (range of response: -50dB to -35dB). Figures F.53 to F.56 show a slight increase in the response during the 85/85 test, which is followed by a decrease during the TS test.

Figures F.57 to F.60 present boxplots for the HF TLC 1GHz measurements versus test time for HASL, benzimidazole, immersion Ag, and immersion Au/Pd, respectively. The boxplots in these figures also show a distinct effect due to coating status. The average HF TLC 500MHz responses by coating status are: none (-12.96dB), parylene (-14.01dB), silicone (-15.64dB), and urethane (-14.06dB). These means are less than those observed at the 500MHz point on the high frequency forward response function. Note the slight increase in the response during the 85/85 test, which is followed by a decrease during the thermal shock test. Figures F.57 to F.60 show a decrease from the 85/85 response levels during the TS test.

Figures F.61 to F.64 present boxplots for the HF TLC RNF measurements versus test time for HASL, benzimidazole, immersion Ag, and immersion Au/Pd, respectively. As with the previous HF TLC measurements, the boxplots in these figures show a distinct effect due to coating status. The average HF TLC RNF responses for parylene, silicone, and urethane coated PWAs are 5.8MHz, 15.4MHz, and 10.7MHz lower than the average response for uncoated PWAs, respectively. However, even though there are distinct differences among the coating conditions, the overall range of HF TLC RNF measurements after 200TS was 630.7MHz to 668.7MHz, which well within the JTP acceptance criterion. Figures F.61 to F.64 show a slight decrease in the response during the 85/85 test, which is followed by an increase during the TS test.

Figures F.65 to F.68 present boxplots for the HF TLC RNR measurements versus test time for HASL, benzimidazole, immersion Ag, and immersion Au/Pd, respectively. The coating effect is not as strong as it was in the previous HF TLC 50MHz, 500MHz, and 1GHz boxplots. These boxplots overlap considerably throughout all figures.

Comparison to JTP Acceptance Criterion. There were seven anomalies that did not meet the JTP acceptance criterion after 200TS, which occurred on seven PWAs. Three of the anomalies were not of sufficient magnitude to be of practical concern. All anomalies are summarized in Table 4.11.

4.8 Leakage Measurements. Four features were included in the design of the LRSTF PWA to specifically check for current leakage: 10-mil pads, PGA socket (PGA-A, PGA-B), and a gull wing component (responses 18 to 21 in Table 1.1). The PGA hole pattern has four concentric squares that are electrically connected by traces on the top layer of the board. Two leakage current measurements were made: (1) between the two inner squares (PGA-A) and (2) between the two outer squares (PGA-B). Solder mask covers the pattern of the PGA-B, allowing a direct comparison of similar patterns with and without solder mask. Rather than an actual PGA device, a socket was used since it provided the same soldering connections as a PGA device. Also, obtaining leakage measurements on an actual PGA is nearly impossible due to complexity of its internal semiconductor circuits.

The JTP acceptance criterion for leakage measurements requires the resistance to be greater than 7.7 when expressed as \log_{10} ohms. The leakage measurements were subjected to GLM analyses, after each phase of the 85/85-TS test sequence (no deltas are calculated for these test measurements). The results of the GLM analyses appear in Tables E.18 to E.21. The model R^2 s from those tables are summarized as follows.

Table 4.11 Failure Analysis Results for HF TLC Circuits after 200 Cycles of Thermal Shock

MSN	Surface Finish	Coating	Flux	Deviation	Failure Analysis Results
HF TLC 50MHz					
663	HASL	Urethane	WS	16.2dB	
778	Immersion Ag	Urethane	LR	-5.3dB	Failure analysis not required
760	Benzimidazole	Urethane	WS	-6.3dB	Failure analysis not required
HF TLC RNR					
769	Immersion Ag	Urethane	LR	30.6dB	
775	Immersion Ag	Urethane	LR	19.4dB	
802	Immersion Ag	Urethane	WS	26.8dB	
915	Immersion Au/Pd	Urethane	WS	11.9dB	Failure analysis not required

Leakage Circuit	Pre-test	Week 1	Week 2	Post	100TS	200TS
10-Mil Pads	80.7%	58.8%	69.1%	72.1%	49.6%	38.3%
PGA-A	41.9%	61.7%	66.4%	43.7%	49.4%	50.5%
PGA-B	41.3%	37.3%	58.0%	32.4%	76.4%	70.9%
Gull Wing	45.4%	28.6%	28.5%	32.8%	41.8%	30.3%

10-Mil Pads. Table E.18 shows the statistically significant coefficients in the GLM in Equation 1.1 for the leakage measurements (\log_{10} ohms) on the 10-mil pads at Pre-test, Weeks 1, 2, and 3, and after 100TS and 200TS. Tables 4.12 to 4.14 give the predicted changes in resistance from the base case for Pre-test, Post-test, and after 200TS for each combination of experimental parameters. Table E.18 shows the GLM base case prediction at Pre-test as 11.06, which is well above the JTP acceptance criterion. All the predicted changes in Table 4.12 are positive so all cases meet the acceptance criterion. The predictions for the empty cells in these tables are the same as that for the base case prediction. Parylene coated PWAs have an average increase of 2.80, silicone has an average increase of 0.44, and urethane has an average increase of 1.52. Note that uncoated PWAs outperform silicone in all but two cases and are on par with urethane coated PWAs. There does not appear to be any significant effect due to either surface finish or flux type, although some their interactions produce different results such as immersion Au/Pd with LR and WS flux on uncoated PWAs.

Table E.18 shows the GLM base case prediction at Post-test as 12.35, which is not only well above the JTP acceptance criterion, but it does not leave much room for improvement. All the predicted changes in Table 4.13 are either zero (no change) or negative (decrease in resistance). Uncoated PWAs with LR give the best overall performance. However, all cases meet the acceptance criterion. Uncoated and silicone coated PWAs have the same performance and both fare slightly better with LR flux. Parylene coated PWAs decrease by one to three orders of magnitude from the base case when WS flux is used. On the other hand, urethane coated PWAs are similar to uncoated PWAs when WS flux is used, but have slightly lower resistance when LR flux is used.

Table E.18 shows the GLM base case prediction at 200TS as 13.76, which is not only well above the JTP acceptance criterion, but it does not leave much room for improvement. All the predicted changes in Table 4.14 are either zero (no change) or negative (decrease in resistance) except for two slight positive increases of 0.09. All cases easily meet the acceptance criterion. Uncoated PWAs have the best overall performance. Parylene is close to the base case. The resistance for both silicone coated and urethane coated PWAs decreases by over an order of magnitude from the base case.

Displays. Figure 4.1 displays boxplots for the leakage measurements on the 10-mil pads versus surface finish after 200TS. These results are in agreement with the conclusions of the GLM analysis at 200TS. Figures F.69 to F.72 present boxplots of the leakage measurements versus test time for each surface finish. The resistance for PWAs processed with WS flux tends to decrease during the 85/85 test in these figures and then increase during the TS test sequence. These figures show that WS flux has an adverse effect on PWAs coated with parylene as the variability of these combinations increases greatly.

Comparison to JTP Acceptance Criterion. There was one anomaly at Post-test and after 200TS that did not meet the JTP acceptance criterion of 7.70. This anomaly occurred on the same PWA (immersion Ag with parylene and WS) at both test times and had resistances of 6.59 and 6.94. This anomaly was due to a burned area resulting from voltage arcing near the input connector (the same cause of an anomaly on the HVLC PTH

Table 4.12 Predicted Changes from the Base Case for the 10-Mil Pads at Pre-test

		No Coating	Parylene	Silicone	Urethane
HASL	LR		3.11	0.63	1.61
	WS	1.91	2.90	0.13	1.41
Benzi	LR	1.08	2.80	0.73	1.61
	WS	1.39	2.67	0.61	1.55
Imm Ag	LR	0.72	2.56	0.58	1.58
	WS	2.63	2.35	0.08	1.38
Im Au/Pd	LR		3.11	0.63	1.61
	WS	1.91	2.90	0.13	1.41

Table 4.13 Predicted Changes from the Base Case for the 10-Mil Pads at Post-test

		No Coating	Parylene	Silicone	Urethane
HASL	LR				-0.72
	WS	-1.06	-2.30	-1.06	-0.62
Benzi	LR				-0.72
	WS	-0.42	-1.66	-0.42	-0.60
Imm Ag	LR				-0.72
	WS	-0.28	-2.97	-1.27	-1.04
Im Au/Pd	LR				-0.72
	WS	-1.06	-2.30	-1.06	-0.62

Table 4.14 Predicted Changes from the Base Case for the 10-Mil Pads after 200TS

		No Coating	Parylene	Silicone	Urethane
HASL	LR			-1.08	-1.63
	WS		-0.93	-1.08	-0.84
Benzi	LR			-1.08	-1.63
	WS		0.09	-1.08	-0.84
Imm Ag	LR			-1.08	-1.63
	WS	-0.46	-1.39	-1.54	-1.30
Im Au/Pd	LR			-1.08	-1.63
	WS	-0.62	0.09	-1.70	-1.46

section) and is unrelated to the board processes (surface finish, coating status, or flux type). As mentioned in Section 4.4, a broken P1 connector on a single PWA at TS200 that did not allow measurements to be recorded for all leakage circuits on that PWA. Since these circuits were normal at TS100, it was assumed that they still functioned properly at TS200.

PGA-A. Table E.19 shows the statistically significant coefficients in the GLM in Equation 1.1 for the leakage measurements (\log_{10} ohms) on PGA-A at Pre-test, Weeks 1, 2, and 3, and after 100TS and 200TS. Tables 4.15 to 4.17 give the predicted changes in resistance from the base case for Pre-test, Post-test, and after 200TS for each combination of experimental parameters.

Table E.19 shows the GLM base case prediction at Pre-test as 10.95, which is well above the JTP acceptance criterion. All the predicted changes in Table 4.15 also meet the acceptance criterion. Parylene coated PWAs have an increase of about an order of magnitude over the base case while urethane has an increase of about 0.70. Results are mixed for silicone with these not showing much change from the base case. Note that uncoated PWAs with WS flux give the best results overall and are about two orders of magnitude higher than uncoated PWAs with LR flux. There does not appear to be any significant effect due to surface finish.

Table E.19 shows the GLM base case prediction at Post-test as 11.82, which is not only well above the JTP acceptance criterion, but it does not leave much room for improvement. All the predicted changes in Table 4.16 are either zero or nearly so (no change) or negative (decrease in resistance). Uncoated PWAs with LR give the

Table 4.15 Predicted Changes from the Base Case for PGA-A at Pre-test

		No Coating	Parylene	Silicone	Urethane
HASL	LR		1.23	0.62	0.67
	WS	2.07	1.02	-0.05	0.71
Benzi	LR		1.23	0.62	0.67
	WS	2.07	1.85	0.88	0.71
Imm Ag	LR		1.23	0.62	0.67
	WS	2.07	1.02	-0.05	0.71
Im Au/Pd	LR		1.23	0.62	0.67
	WS	2.07	1.02	-0.05	0.71

Table 4.16 Predicted Changes from the Base Case for PGA-A at Post-test

		No Coating	Parylene	Silicone	Urethane
HASL	LR		-0.75	-1.75	-1.03
	WS	-1.40	-2.15	-1.58	-1.10
Benzi	LR		-0.75	-0.49	-1.03
	WS	-1.40	-2.15	-0.32	-1.10
Imm Ag	LR		-0.75	-0.11	-1.03
	WS	-1.40	-2.15	-1.34	-1.10
Im Au/Pd	LR		-0.75	0.06	-1.03
	WS	-1.40	-2.15	-1.64	-1.10

Table 4.17 Predicted Changes from the Base Case for PGA-A after 200TS

		No Coating	Parylene	Silicone	Urethane
HASL	LR				-2.35
	WS	-1.06	0.17	-1.06	-1.78
Benzi	LR	-0.80	0.36	0.03	-2.03
	WS	-1.86	0.53	-1.03	-1.46
Imm Ag	LR				-2.35
	WS	-1.06	0.17	-1.06	-1.78
Im Au/Pd	LR				-2.35
	WS	-1.06	0.17	-1.06	-1.78

best overall performance. However, all cases meet the acceptance criterion. The resistance for uncoated PWAs is 1.40 orders of magnitude lower than the base case with WS flux, which is just opposite of the situation at Pre-test. Parylene coated PWAs decrease by over two orders of magnitude from the base case when WS flux is used. Results are mixed for silicone. Resistance is about an order of magnitude lower than the base case for all urethane cases. There does not appear to be any significant effect due to surface finish.

Table E.19 shows the GLM base case prediction at 200TS as 13.22, which is not only well above the JTP acceptance criterion, but it does not leave much room for improvement. Almost all predicted changes in Table 4.17 are either zero or nearly so (no change) or negative (decrease in resistance). However, all cases easily meet the acceptance criterion. Uncoated and parylene coated PWAs have almost identical values with LR flux, but parylene is an order of magnitude better with WS flux. The resistance for silicone coated PWAs is similar to uncoated PWAs for all cases. The resistance for urethane coated PWAs decreases by 1.5 to 2.3 orders of magnitude relative to the base case for all surface finish/flux combinations.

Displays. Figure 4.2 displays boxplots for the leakage measurements on PGA-A versus surface finish after 200TS. These results are in agreement with the conclusions of the GLM analysis at 200TS. Figures F.73 to F.76 present boxplots of the leakage measurements versus test time for each surface finish. These boxplots show greater variability for uncoated PWAs during TS and for parylene at Pr-test. Resistance increases for all PWAs during TS.

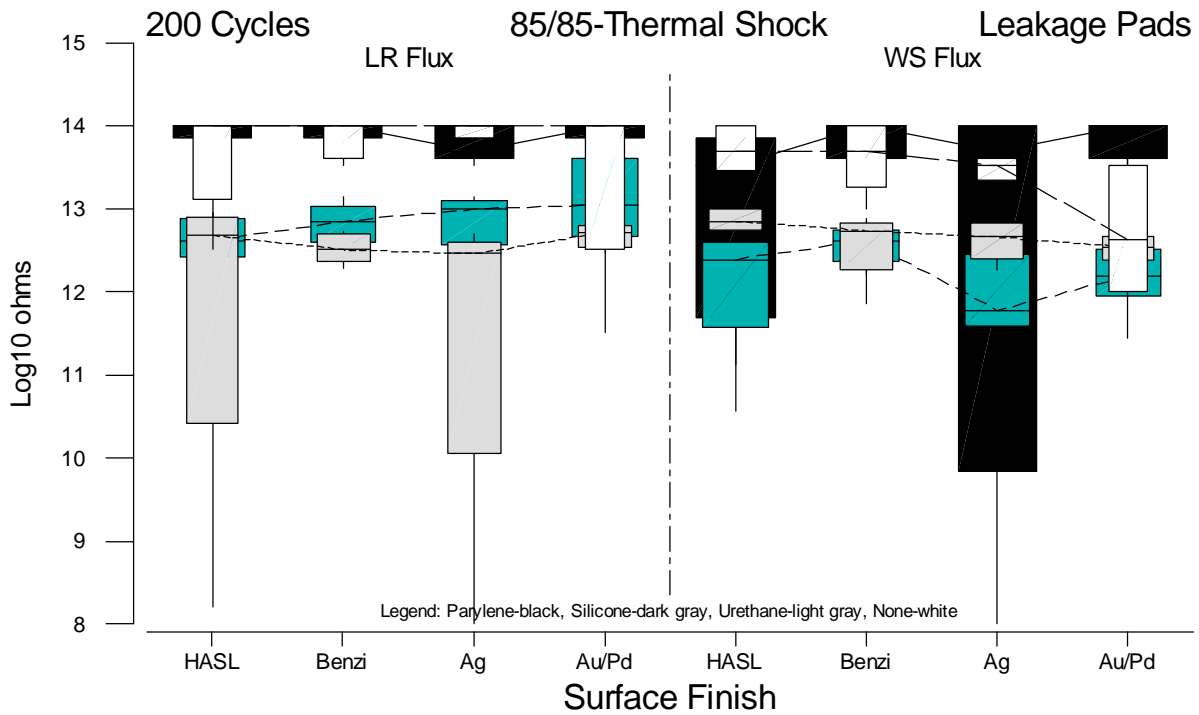


Figure 4.1 Boxplot Displays for the 10-mil Pads by Coating Status and Flux Type versus Surface Finish after 200 Cycles of Thermal Shock

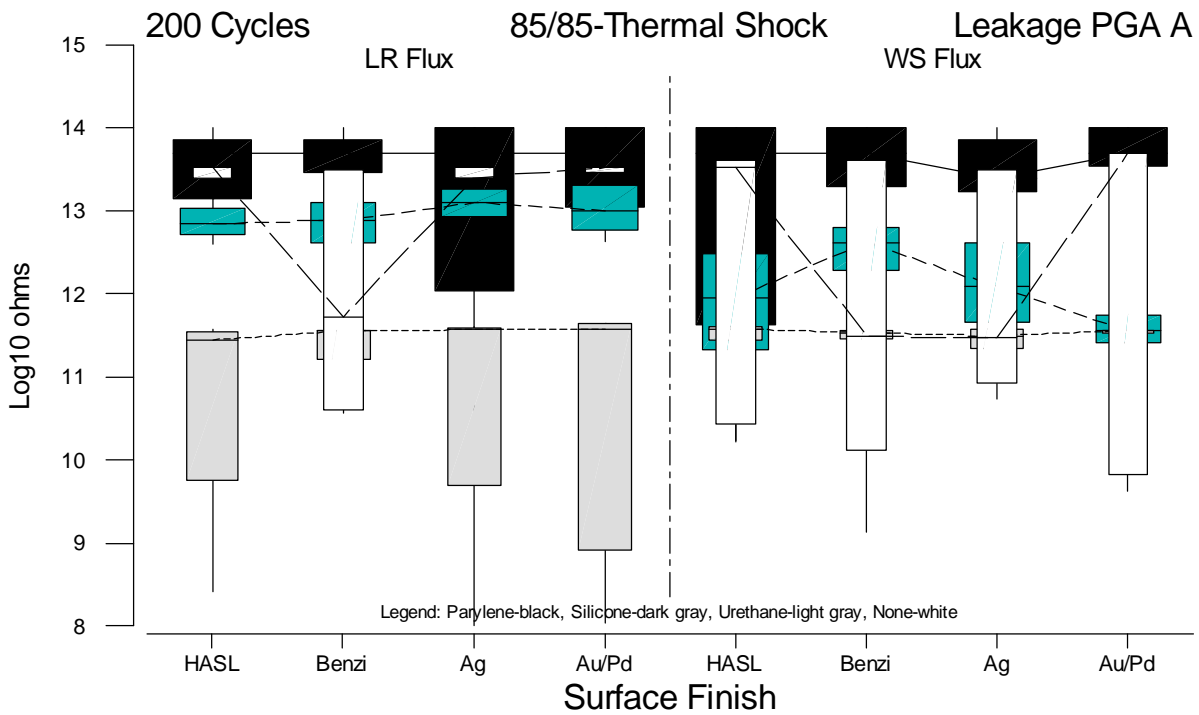


Figure 4.2 Boxplot Displays for PGA-A by Coating Status and Flux Type versus Surface Finish after 200 Cycles of Thermal Shock

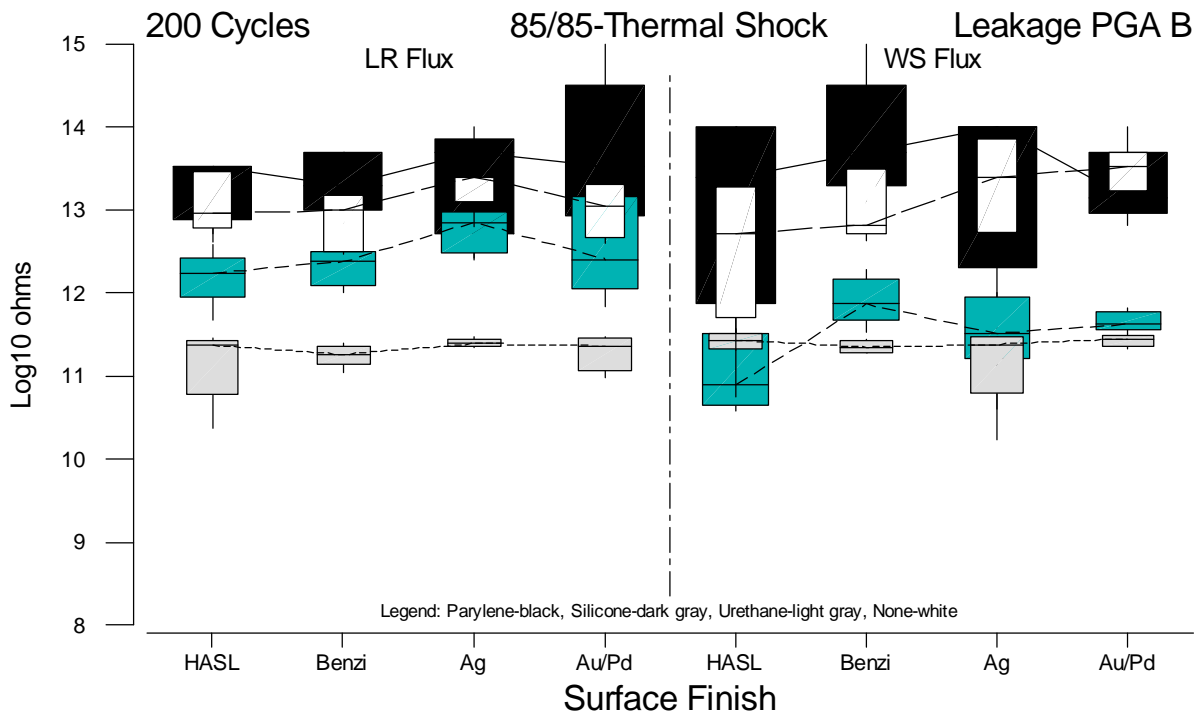


Figure 4.3 Boxplot Displays for PGA-B by Coating Status and Flux Type versus Surface Finish after 200 Cycles of Thermal Shock

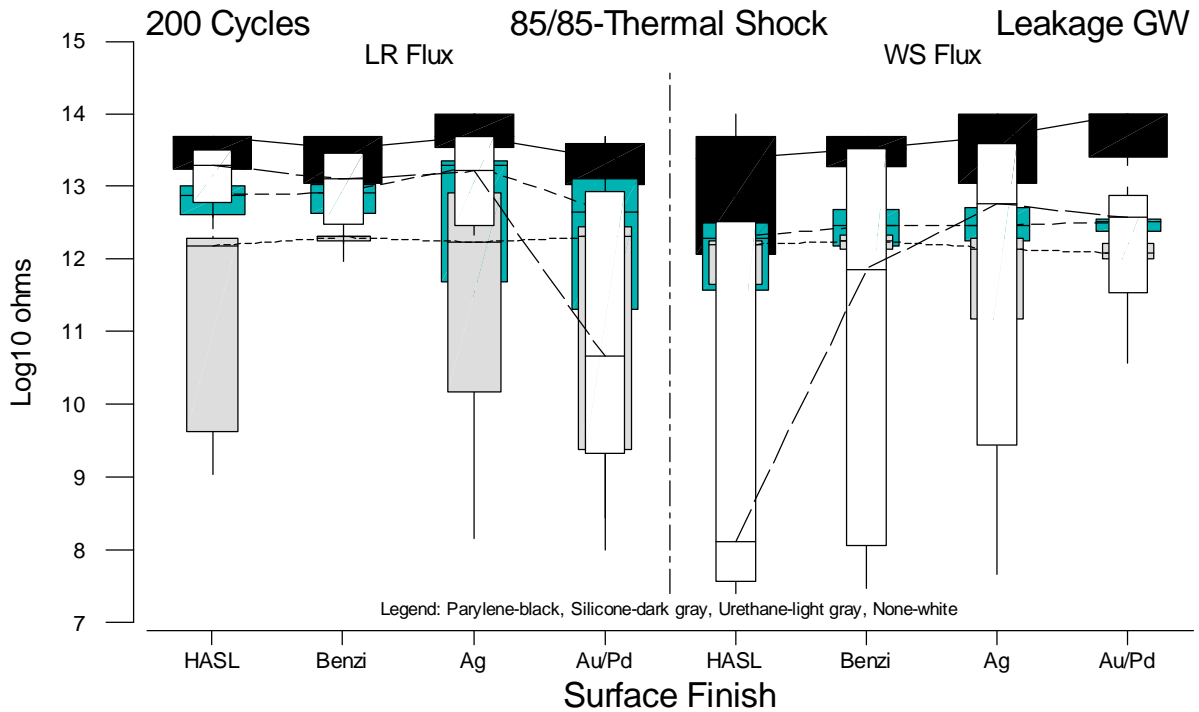


Figure 4.4 Boxplot Displays for the Gull Wing by Coating Status and Flux Type versus Surface Finish after 200 Cycles of Thermal Shock

Table 4.18 Predicted Changes from the Base Case for PGA-B at Pre-test

		No Coating	Parylene	Silicone	Urethane
HASL	LR		1.37	0.60	0.79
	WS	2.45	1.11	0.37	0.73
Benzi	LR		1.37	0.60	0.79
	WS	2.45	1.11	0.37	0.73
Imm Ag	LR		1.37	0.60	0.79
	WS	2.45	1.11	0.37	0.73
Im Au/Pd	LR		1.37	0.60	0.79
	WS	2.45	1.11	0.37	0.73

Table 4.19 Predicted Changes from the Base Case for PGA-B at Post-test

		No Coating	Parylene	Silicone	Urethane
HASL	LR		-1.03	-0.47	-0.72
	WS		-1.03	-0.47	-0.72
Benzi	LR		-1.03	-0.47	-0.72
	WS	0.48	-0.55	0.01	-0.24
Imm Ag	LR	0.65	-0.38	0.18	-2.33
	WS	0.65	-0.38	0.18	-0.64
Im Au/Pd	LR	0.59	-0.44	0.12	-0.13
	WS	0.59	-0.44	0.12	-0.13

Table 4.20 Predicted Changes from the Base Case for PGA-B after 200TS

		No Coating	Parylene	Silicone	Urethane
HASL	LR		0.32	-0.62	-1.77
	WS		0.32	-1.53	-1.77
Benzi	LR		0.32	-0.62	-1.77
	WS		0.32	-1.53	-1.77
Imm Ag	LR		0.32	-0.62	-1.77
	WS		0.32	-1.53	-1.77
Im Au/Pd	LR		0.32	-0.62	-1.77
	WS		0.32	-1.53	-1.77

Comparison to JTP Acceptance Criterion. There was one anomalous measurement for PGA-A at Post-test, but it returned to normal after 200TS.

PGA-B. Table E.20 shows the statistically significant coefficients in the GLM in Equation 1.1 for the leakage measurements (\log_{10} ohms) on PGA-B at Pre-test, Weeks 1, 2, and 3, and after 100TS and 200TS. Solder mask covers the pattern of PGA-B allowing a direct comparison of similar patterns with and without solder mask. Tables 4.18 to 4.21 give the predicted changes in resistance from the base case for Pre-test, Post-test, and after 200TS for each combination of experimental parameters.

Table E.20 shows the GLM base case prediction at Pre-test as 10.62, which is well above the JTP acceptance criterion. All the predicted changes in Table 4.18 are positive so all cases meet the acceptance criterion. Parylene coated PWAs have an increase of about an order of magnitude over the base case while urethane has an increase of about 0.75. Results are mixed for silicone with these not showing much change from the base case. Note that uncoated PWAs with WS flux give the best results overall and are about 2.5 orders of magnitude higher than uncoated PWAs with LR flux, which is similar to the behavior of PGA-B. There does not appear to be any significant effect due to surface finish.

Table E.20 shows the GLM base case prediction at Post-test as 11.03, which is well above the JTP acceptance criterion. Almost all the predicted changes in Table 4.19 are less than an order of magnitude different from the base case. A notable exception occurs for immersion Ag coated with urethane and processed with LR flux, which

has a predicted resistance approximately 2.3 orders of magnitude less than the base case (but still meets the JTP acceptance criterion). Uncoated PWAs with LR give the best overall performance. However, all cases meet the acceptance criterion. There does not appear to be any significant effect due to surface finish.

Table E.20 shows the GLM base case prediction at 200TS as 13.08, which is not only well above the JTP acceptance criterion, but it does not leave much room for improvement. Note that all uncoated cases are the same as the base case in Table 4.21. The predicted resistance for parylene is approximately 0.3 orders of magnitude higher than the base for all surface finish/flux combinations. The predicted resistance for silicone is approximately 0.6 orders of magnitude less than the base case when LR flux is used and 1.5 orders of magnitude less when WS flux is used. Urethane coated PWAs have a predicted resistance of 1.77 orders of magnitude lower than the base case for all cases. There does not appear to be any significant effect due to surface finish.

Displays. Figure 4.3 displays boxplots for the leakage measurements on PGA-B versus surface finish after 200TS. These results are in agreement with the conclusions of the GLM analysis at 200TS. Figures F.77 to F.80 present boxplots of the leakage measurements versus test time for each surface finish. These boxplots show the lower resistance after 200TS for silicone coated PWAs, which correlates with the GLM results in Table 4.18. The resistance increases for all PWAs during TS. Parylene coated PWAs exhibit the greatest variability in many cases.

Comparison to JTP Acceptance Criterion. All PGA-B leakage measurements met the JTP acceptance criterion after 200TS.

Gull Wing. Table E.21 shows the statistically significant coefficients in the GLM in Equation 1.1 for the leakage measurements (\log_{10} ohms) on the gull wing at Pre-test, Weeks 1, 2, and 3, and after 100TS and 200TS. Tables 4.21 to 4.23 give the GLM predicted changes in resistance from the base case for Pre-test, Post-test, and after 200TS for each combination of experimental parameters.

Table E.21 shows the GLM base case prediction at Pre-test as 11.67, which is well above the JTP acceptance criterion. All predicted changes in Table 4.21 meet the acceptance criterion. Parylene coated PWAs have an increase of about 1.4 orders of magnitude over the base case. Immersion Ag has an increase in resistance of about 0.6 orders of magnitude for uncoated and silicone coated PWAs. Immersion Ag also has an increase of about 0.6 orders of magnitude for urethane with LR flux is used, but experiences a decrease of about an order of magnitude with WS flux. There does not appear to be any significant effect due to surface finish.

Table E.22 shows the GLM base case prediction at Post-test as 11.81, which is well above the JTP acceptance criterion. All predicted changes in Table 4.22 are negative, but still meet the acceptance criterion. Use of WS flux lowers resistance relative to the base case for all surface finishes. Use of LR flux lowers resistance for immersion Au/Pd and for all parylene cases. There does not appear to be any significant effect due to surface finish.

Table E.23 shows the GLM base case prediction at 200TS as 13.12, which is not only well above the JTP acceptance criterion, but it does not leave much room for improvement. Hence, most predicted changes in Table 4.23 are negative, but still meet the JTP acceptance criterion. WS flux has a negative effect on resistance for uncoated, silicone and urethane coated PWAs, but has a slight positive influence on PWAs coated with parylene. Urethane coating has a negative effect on resistance for all cases. Immersion Au/Pd with LR flux also has a negative effect on resistance for all but one case. There does not appear to be any significant effect due to surface finish.

Displays. Figure 4.4 displays boxplots for the leakage measurements on gull wing versus surface finish after 200TS. These results are in agreement with the conclusions of the GLM analysis at 200TS. Figures F.81 to F.84 present boxplots for the leakage measurements on the gull wing versus test time for HASL, benzimidazole, immersion Ag, and immersion Au/Pd, respectively. These boxplots show that uncoated PWAs processed with WS flux have greater variability than coated PWAs for all surface finishes except immersion Au/Pd. In this latter case, uncoated PWAs still have the greatest variability, but for those PWAs processed with LR flux.

Comparison to JTP Acceptance Criterion. There were three anomalous GW leakage measurements that did not meet the JTP acceptance criterion after 200TS. These anomalies were just under the lower limit (7.70) at 7.67, 7.47, and 7.40 and were not deemed to be of practical concern.

Table 4.21 Predicted Changes from the Base Case for the Gull Wing at Pre-test

		No Coating	Parylene	Silicone	Urethane
HASL	LR		1.45		
	WS		1.45		
Benzi	LR		1.45		
	WS		1.45		
Imm Ag	LR	0.63	1.32	0.63	0.63
	WS	0.63	1.32	0.63	-1.01
Im Au/Pd	LR		1.45		
	WS		1.45		

Table 4.22 Predicted Changes from the Base Case for the Gull Wing at Post-test

		No Coating	Parylene	Silicone	Urethane
HASL	LR		-0.74		
	WS	-2.08	-1.19	-0.24	-0.27
Benzi	LR		-0.74		
	WS	-2.08	-1.19	-0.24	-0.27
Imm Ag	LR		-0.74		
	WS	-2.08	-1.19	-0.24	-0.27
Im Au/Pd	LR	-0.72	-1.46	-0.72	-0.72
	WS	-0.39	-1.30	-0.34	-0.33

Table 4.23 Predicted Changes from the Base Case for the Gull Wing after 200TS

		No Coating	Parylene	Silicone	Urethane
HASL	LR				-1.29
	WS	-2.07	0.20	-0.88	-1.21
Benzi	LR				-1.29
	WS	-2.07	0.20	-0.88	-1.21
Imm Ag	LR				-1.29
	WS	-2.07	0.20	-0.88	-1.21
Im Au/Pd	LR	-0.80	-0.80	-0.80	-2.09
	WS	-1.54	0.73	-0.35	-0.68

4.9 Stranded Wires. Two stranded wires were hand soldered on the LRSTF PWA (responses 22 and 23 in Table 1.1). One wire was soldered into plated through holes and the other was soldered to two terminals. The JTP acceptance criterion requires changes in voltage to be within 0.356V of their Pre-test measurements.

Pre-test measurements for both stranded wires were subjected to GLM analyses, as were the deviations for Delta 1 to Delta 5. The results of the GLM analyses appear in Tables E.22 and E.23. The model R^2 s in those tables are summarized as follows.

Circuit	Pre-test	Week 1	Week 2	Post	100TS	200TS
Stranded Wire 1	7.3%	17.8%	17.5%	13.8%	19.5%	19.6%
Stranded Wire 2	35.3%	8.0%	1.6%	12.0%	9.5%	6.1%

These R^2 values are quite small and imply that the experimental parameters do not differ significantly from the base case in terms of their impact on the stranded wire voltages.

Displays. Figures F.85 to F.88 present boxplots for the voltage measurements (mV) on stranded wire 1 versus test time for HASL, benzimidazole, immersion Ag, and immersion Au/Pd, respectively. The boxplots overlap considerably throughout. Figures F.89 to F.92 present boxplots for the voltage measurements (mV) on stranded wire 2 versus test time for HASL, benzimidazole, immersion Ag, and immersion Au/Pd, respectively. The boxplots also overlap considerably throughout.

Comparison to JTP Acceptance Criterion. The largest observed changes after 200TS for stranded wires 1 and 2 were only 0.006V and 0.007V, respectively, which are well below the JTP acceptance criterion of 0.356V.

4.10 Summary of 85/85 and Thermal Shock Results. Detailed results of the electrical performance of 160 LRSTF PWAs after three weeks exposure to an 85/85 test environment followed by 200 cycles of thermal shock have been presented in this section. These PWAs were each tested four times for the 85/85 environment: Pre-test and after each week of exposure. The PWAs in the TS test were tested after 100 cycles and 200 cycles. At each test time, 3680 electrical measurements were recorded and compared to the JTP acceptance criteria.

Summary of the Yields by Surface Finish and Coating Status. A summary of the yields of the circuits relative to the JTP acceptance criteria at the end of Post-test and 200TS is given in Table 4.24.

Table 4.24 Yields for Circuits Relative to the JTP Acceptance Criteria at the Conclusion of the 85/85—Thermal Shock Test Sequence

Circuitry	Post 85/85	200TS
HCLV	319/320 = 99.7%	319/320 = 99.7%
HVLC	310/320 = 96.9%	310/320 = 96.9%
HSD	320/320 = 100.0%	320/320 = 100.0%
HF LPF	954/960 = 99.4%	948/960 = 98.8%
HF TLC	796/800 = 99.5%	795/800 = 99.4%
ON	628/640 = 98.1%	636/640 = 99.4%
SW	320/320 = 100.0%	320/320 = 100.0%
Totals	3647/3680 = 99.1%	3646/3680 = 99.1%

Tables 4.25 and 4.26 breakdown the overall yield summaries in Table 4.24 by surface finish and coating status, respectively. Before a discussion of that breakdown is presented, the reader needs to be aware that the summary in Table 4.24 is based on the total number of anomalies and not on the number of PWAs having anomalies. Multiple anomalies on a single PWA influence the overall yield for the affected surface finish even though there may be some common source causing the multiple anomalies. Thus, a PWA with three HF LPF anomalies produces three anomalies for the respective surface finish even though they all occurred on a single PWA.

With that warning as a backdrop, the summary in Table 4.24 shows that all circuits had high yields at the conclusion of the 85/85-TS test sequence. Table 4.25 shows that benzimidazole has the highest overall yield at both Post 85/85 and 200TS while immersion Ag has the lowest overall yield. However, all surface finishes are quite close with the total yields ranging from 98.6% to 99.6% at Post 85/85 and from 98.5% to 99.7% at 200TS.

Table 4.25 Yields by Surface Finish Relative to the JTP Acceptance Criteria at the Conclusion of the 85/85—TS Test Sequence

Circuitry	Post 85/85				200TS			
	HASL	Benzi	Imm Ag	Imm Au/Pd	HASL	Benzi	Imm Ag	Imm Au/Pd
HCLV	100.0%	100.0%	100.0%	98.8%	100.0%	100.0%	98.8%	100.0%
HVLC	95.0%	97.5%	97.5%	97.5%	95.0%	98.8%	96.3%	97.5%
HSD	100.0%	100.0%	100.0%	100.0%	100.0%	100.0%	100.0%	100.0%
HF LPF	100.0%	100.0%	98.3%	99.2%	100.0%	100.0%	98.3%	96.7%
HF TLC	100.0%	99.5%	98.5%	100.0%	99.5%	99.5%	98.0%	99.5%
ON	96.3%	99.4%	97.5%	99.4%	99.4%	99.4%	98.8%	100.0%
SW	100.0%	100.0%	100.0%	100.0%	100.0%	100.0%	100.0%	100.0%
Totals	98.9%	99.6%	98.6%	99.3%	99.3%	99.7%	98.5%	98.8%

Table 4.26 Yields by Coating Status Relative to the JTP Acceptance Criteria at the Conclusion of the 85/85—TS Test Sequence

Circuitry	Post 85/85				200TS			
	Uncoated	Parylene	Silicone	Urethane	Uncoated	Parylene	Silicone	Urethane
HCLV	100.0%	100.0%	100.0%	98.8%	100.0%	100.0%	100.0%	98.8%
HVLC	95.0%	97.5%	97.5%	97.5%	91.3%	97.5%	98.8%	100.0%
HSD	100.0%	100.0%	100.0%	100.0%	100.0%	100.0%	100.0%	100.0%
HF LPF	100.0%	100.0%	98.3%	99.2%	99.2%	97.9%	97.9%	100.0%
HF TLC	100.0%	99.5%	98.5%	100.0%	100.0%	100.0%	100.0%	96.5%
ON	96.3%	99.4%	97.5%	99.4%	98.1%	99.4%	100.0%	100.0%
SW	100.0%	100.0%	100.0%	100.0%	100.0%	100.0%	100.0%	100.0%
Totals	98.9%	99.6%	98.6%	99.3%	98.7%	99.1%	99.3%	99.1%

The summary in Table 4.26 shows that all coating categories are also quite close with the total yields ranging from 98.6% to 99.6% at Post 85/85 and from 98.7% to 99.3% at 200TS. Perhaps the most surprising result in Table 4.26 is how well uncoated PWAs fared. This group was slightly better than silicone coated PWAs at Post 85/85 and was only 0.7% behind the best performance recorded by parylene. Uncoated PWAs have the lowest yield at 200TS, but again are only 0.6% behind the best performance recorded by silicone. The reader is again cautioned to take care in interpreting these results, as all cases are quite close.

Summary of Anomalies by PWA. At the conclusion of the 85/85 test, there were 33 anomalous measurements that did not meet the JTP acceptance criteria. Twenty of these 33 anomalies carried over to 200TS. There were 14 new anomalies at TS200, bringing the total to 34 at the conclusion of the 85/85-TS test sequence. These 34 anomalies occurred on 24 PWAs with the number of anomalies per PWA summarized as follows.

Number of Anomalies	Frequency
0	136
1	16
2	6
3	2
	160

Of the 34 anomalies at 200TS, 21 were severe enough to be candidates for failure analysis. These 21 anomalies occurred on 16 PWAs with eight of the 21 anomalies occurring on just three PWAs. The 16 PWAs with severe anomalies included all surface finishes, coating status, and flux as shown in Table 4.25.

The summaries in Tables 4.24 and 4.25 do not include 27 HSD circuits that did not respond after 200TS since these are typically due to component or trace damage as previously discussed in Section 4.5. Failure analysis revealed that all the damage sustained in the HSD section was due to electrical overstress (EOS), which damaged either the active components or the circuit traces. The source of the EOS was likely from the adjacent Other Networks (leakage current) section of the PWA, which was biased with 100V.

The 25 damaged HSD circuits occurred on 18 PWAs, which are summarized by surface finish, coating status, and flux as shown in Table 4.26. This summary shows that the damaged components and traces were spread over all surface finishes, coating conditions, and flux types.

Table 4.25 Joint Summary of the 16 PWAs that are Candidates for Failure Analysis after 200TS

		No Coating	Parylene	Silicone	Urethane	Totals
HASL	LR	1	1			1
	WS	1			1	3
Benzimidazole	LR					
	WS	1				1
Immersion Ag	LR	1			2	3
	WS	1	1		1	3
Immersion Au/Pd	LR	3	1		1	4
	WS			1		1
Totals		8	3	1	4	16

Table 4.26 Summary of the 18 PWAs with Damaged HSD Components or Circuit Traces

		No Coating	Parylene	Silicone	Urethane	Totals
HASL	LR				1	1
	WS	2	1	1	1	5
Benzimidazole	LR		1			1
	WS	1	1		1	3
Immersion Ag	LR				1	1
	WS	1	1			2
Immersion Au/Pd	LR	2	1		1	4
	WS	1				1
Totals		7	5	1	5	18

References

1. Joint Group on Acquisition Pollution Prevention (JG-APP) Joint Test Protocol CC-P-1-1 for Validation of Alternatives to Lead-Containing Surface Finishes, for Development of Guidelines for Conformal Coating Usage, and for Qualification of Low-VOC Conformal Coatings (1998).
2. Iman, R. L. (1994). **A Data-Based Approach to Statistics**, Duxbury Press.

